



# The Effect of Post-Earthquake Fire on the Performance of Steel Moment Frames Subjected to Different Ground Motion Intensities

Peyman Pourkaramat<sup>1</sup> · Vahed Ghiasi<sup>1</sup> · Benyamin Mohebi<sup>2</sup>

Received: 9 June 2020 / Accepted: 30 May 2021 / Published online: 6 June 2021  
© Korean Society of Steel Construction 2021

## Abstract

In this paper, post-earthquake fire modeling was studied in steel structures with different levels of ground motion intensity. Three-story structure modeling was implemented under post-earthquake fire by using the OpenSees software. The performance of the structure was investigated under different levels of ground motion intensity to the level of life safety. The structure was subjected to seismic and thermal analysis by applying standard fire load up to 880 s of fire. The 9-point thermal gradient for beam and column profiles under heat was analyzed by heat transfer analysis in the software. By comparing obtained results from the seismic analysis and post-earthquake fire analysis, it can be seen that for different levels of ground motion intensity, the behavior of the structure is different when it is exposed to post-earthquake fire than being exposed to the earthquake alone, which can affect the performance-based design of the structure. Therefore, in the design of structures, the effect of post-earthquake fire should be taken into account, considering the seismic zone of the structure and the time required to extinguish the fire.

**Keywords** Post-earthquake fire · Heat transfer · Thermal analysis · Performance-based design

## 1 Introduction

Post-Earthquake Fire (PEF) is considered as one of the most catastrophic events in urban areas which may result significant financial and life losses. In severe earthquakes causing happens, which cause massive damage to the buildings, roads, and bridges, there is a high chance of PEF occurrence that makes the process of rescuing the people very difficult.

Study on PEF events reveals that post-earthquake fires have occurred in different earthquakes, for example, in the earthquake that happened in Tokyo, Japan in 1923, fire affected an area of approximately 35 square kilometers, or in the earthquake that occurred in Mexico City, Mexico in 1985 fire destroyed many buildings. There are other cases that all indicate PEF as a real threat which requires conduction of research, study, and presentation of solution (Khorasani & Garlock, 2017).

According to design regulations and standards, structures are designed for gravity and lateral loads, and the simultaneous combination of earthquake and fire loads has not been considered.

On the other hand, most existing conventional buildings have not been designed for post-earthquake thermal loading, and there is a high likelihood of the rapid collapse of damaged buildings in post-earthquake fire.

It is necessary to take PEF into account of a design scenario in performance-based concepts in severe earthquakes considering past experiences with post-earthquake fires.

The structure should be designed for different levels of production using a design philosophy based on the performance of the structural members, such as Operational (o), Immediate Occupancy (Io), Life Safety (LS), and Collapse Prevention (CP).

Post-earthquake fire causes changes in the performance level of design for a given structure. Therefore, using non-linear analyses and considering the issue of PEF, one can investigate the exact behavior of the structure.

Due to the reasons mentioned in various researches, the behavior of steel structures has been studied under fire and post-earthquake fire.

✉ Vahed Ghiasi  
v.ghiasi@malayeru.ac.ir

<sup>1</sup> Department of Civil Engineering, Malayer University, Malayer, Iran

<sup>2</sup> Department of Civil Engineering, Imam Khomeini International University, Qazvin, Iran

Tomecek and Milke (1993), in a two-dimensional study, showed that the steel columns protected by fire-resistant materials were more resistant than unprotected steel columns. They also showed that even losing 4% of the protective layer can significantly reduce the fire resistance of the columns up to 40%.

Ryder et al. (2002) investigated the effect of loss of fire protection materials on the relative strength of steel columns in a three-dimensional environment. Initially, fully protected columns were subjected to a 90 min fire to transfer the temperature to another surface. Then, protective layers were randomly removed from the column, and unprotected columns were exposed to fire. They showed that, even if the protective layer is removed from a small area, a significant decrease will occur in steel column resistance against fire.

Della Corte et al. (2003) investigated bending frames of unprotected steel and their response to post-earthquake fires. They calculated geometric nonlinear behavior (P- $\Delta$  effect), full plastic-elastic behavior of assuming steel, and degree of fire resistance using numerical methods. They analyzed the fire for the two states of pre and post-earthquake. They demonstrated that the relative displacement of the stories is an essential parameter in fire resistance. Their results showed that type of failure, as well as the PEF resistance, strongly depend on fire scenarios and gravity loads.

Zaharia and Pintea (2009) studied post-earthquake fires on two different steel frames designed for two earthquake return periods of 2475 and 475 years. The frame designed for a return period of 2475 years was in the elastic range of the Pushover analysis, but the frame designed under weaker earthquake (a return period of 475 years) underwent significant inter-story relative displacement. Then, they carried out a fire analysis on both frames and proved that the buildings that had experienced deformation against earthquakes were less resistant to fire than those that did not have a pre-fire deformation.

Wang and Li (2009) investigated the effect of fire on the steel structure and illustrated that the relative strength of steel columns that their protective layers have been damaged by fire is much less than those that are fully protected against fire.

Memari et al. (2014) investigated the performance of the steel bending frame with reduced connections at the beam cross-section following a post-earthquake fire. In this study using ABAQUS software (Systèmes, 2007), three bending frames of 3, 9 and 20 floors under 5 near-field earthquakes and 5 far-field earthquakes for two one-thirds and two-thirds height building fire scenarios under Post-earthquake fires were investigated. The result of this research is to compare the performance level of the structures in the scenarios with the performance level under earthquake.

Khorasani et al. (2015) investigated the PEF modeling using the OpenSees software (Mazzoni et al., 2006). They

made a comparison between structural modeling in the OpenSees software with modified thermal materials and the SAFIR software (Franssen & Gernay, 2019) for two steel frames and steel columns. After validation, the results of the 9-story steel frame were evaluated for cases of fire-only and PEF. Their results showed that, by modeling the structure with modified thermal materials in the OpenSees software, the behavior of the structure could be modeled with high accuracy in the PEF.

Behnam (2016) investigated the PEF on a 7-story irregular steel building at an elevation. This frame was designed initially under an earthquake with the acceleration of 0.35 g, and after applying the earthquake to target displacement and thermal loading on it, the results were compared to the regular frame. Irregular structures at elevation were found to be more sensitive to PEF loads than regular structures.

Behnam (2018), in another study, investigated the failure of tall steel moment frame structures under natural fire, focusing on the possibility of structural failure in the cooling phase, for a 10-story steel moment frame with span lengths of 6 and 7.5 m and the opening ratio of 0.02–0.2.

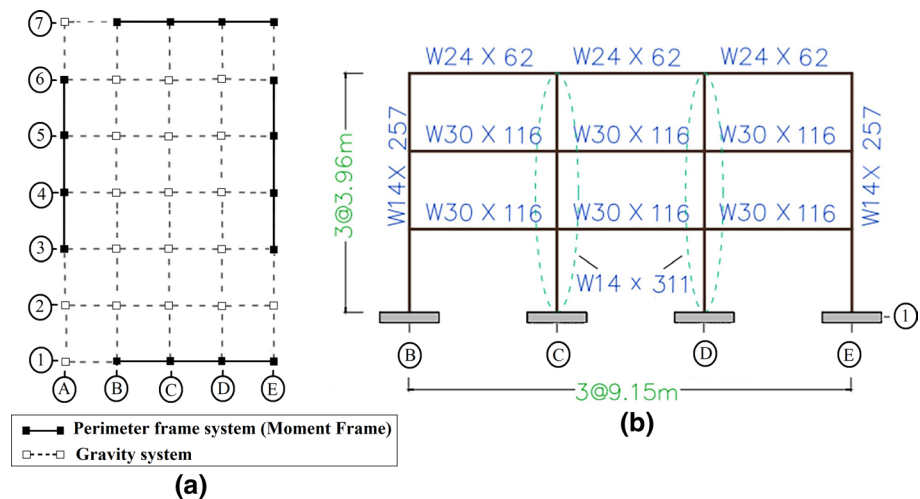
Using SAFIR software, it was shown that, in the structures designed for dead and live loads, although the structures are sufficiently resistant to fire during the heating phase, they are vulnerable in the cooling period especially under opening ratios more than 10% of the surface area. In contrast, if the structure is designed under dead, live, and earthquake loads, it will not fail during the heating and cooling phases even when the opening is 20% of the surface area.

In this study, due to the importance of design based on the performance of structures, a 3-story moment steel frame structure under different scales of earthquake accelerograms to 880 s of post-earthquake fire to the life safety level is studied. A range of the pseudo-acceleration spectrum component is determined in the period of the first mode of structure  $S_a(T_1)$  that if the structure under the earthquake that creates this acceleration spectrum component remains at the level of life safety, there is no need to check PEF for that duration of fire, and it will also remain at the level of life safety under PEF.

## 2 Post-Earthquake Fire Modeling

In this study, 3-story steel SMRF (Special Moment Resisting Frame) structure with a regular plan and the perimeter frame system was considered. This structure has been designed for seismic conditions in Los Angeles, seismic zone 4 defined in UBC94 (1994), according to the post-Northridge seismic design criteria and is part of the SAC steel project (Venture & Sacramento, 1994). More details about this structure are available in FEMA-355C (Krawinkler, 2000). Figure 1

**Fig. 1** Specifications of three-story SAC frame. **a** Plan; **b** Elevation



shows the specifications of the beams and columns of this structure.

The structure was loaded under two simulations. In the first model, the structure was analyzed using different scaled earthquakes. In the second model, the structure was subjected to different sized earthquakes, and then, the behavior of the structure was studied by considering the 60 s of free vibration after the earthquake for damping and applying fire load. For modeling of the PEF, the following steps are taken:

- (1) Selecting an earthquake scenario as an input load for the seismic design that involves selecting an earthquake mapping acceleration scale or equivalent seismic load.
- (2) Selection of fire scenario as an input load for structural analysis against fire, including the selection of fire compartment position in the frame, defining complete temperature–time curve of fire, conducting heat transfer analysis to develop temperature–time curve on structural elements exposed to fire.
- (3) Performing seismic structural analysis
- (4) Modification of constraints in the model to allow thermal expansion of the points (in step 3, horizontal displacements of the nodes on the ceiling are interconnected to act as a diaphragm during the earthquake, and the constraints on the ceiling should be released during fire analysis (Khorasani et al., 2015)).
- (5) Performing structural-fire analysis.

In previous studies, the PEF modeling has been done mostly in a way that, firstly, the structure was analyzed by pushover seismic analysis using SAP software (2009). Then, structural fire analysis was done by transferring displacement caused by the earthquake to SAFIR software (Franssen & Gernay, 2019).

In this research, the perimeter moment frame is modeled in two-dimensional according to the plan in Fig. 1 and the

effect of the ceiling on the bending stiffness of the beams is neglected.

Fire is considered simultaneously in each scenario, but the application of fire load in the columns is different. As in the corner column it is exposed to fire on two sides and the middle and outer column on the side of the gravity column it is considered as three sides exposed to fire, and the general behavior of the structure is studied by examining the relative displacement in the stories.

### 3 Thermal and Mechanical Properties of Steel

Usually with increasing temperature, the yield stress of steel decreases. In steel, the decrease in mechanical properties is between 300 °C (modulus of elasticity) and 500 °C (compressive strength) Behnam (2017). Figure 2 shows the thermal and mechanical properties of steel at various temperatures.

### 4 Structural Modeling

In this research, the Open System for Earthquake Engineering Simulatio (OpenSees was used to model and perform related analyses.

As currently, the dispBeamColumnThermal element is only available in the OpenSees software for heat analysis in beam-columns (Khorasani et al., 2015), therefore, in the modeling of the columns, nonlinear behavior of the columns was modeled as distributed plasticity using beam-column elements with displacement formulation.

Since stiffness is linear in elements with displacement formulation, the columns were divided into 10 segments to increase accuracy and achieve exact curvature. Five

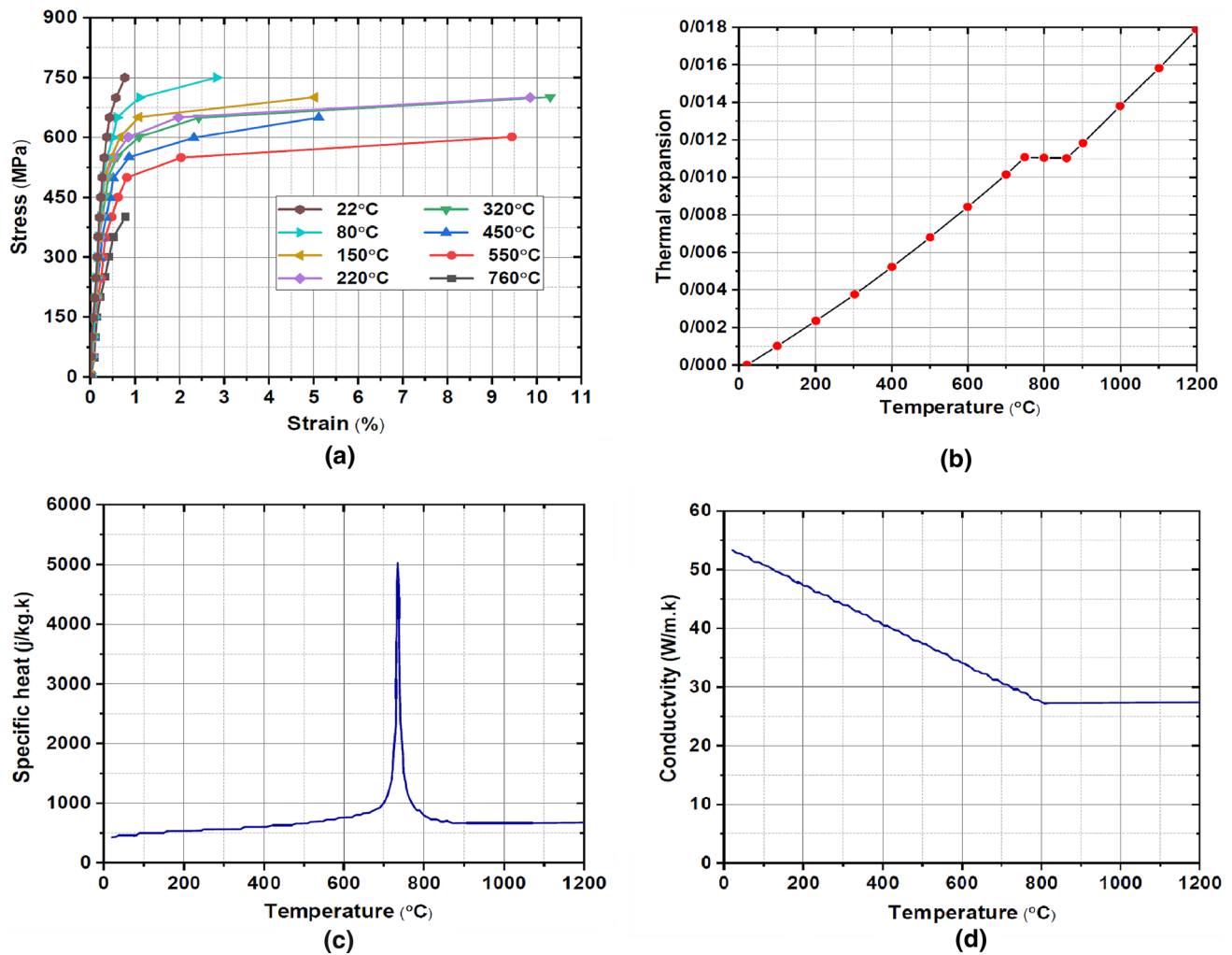


**Fig. 2** a Strain stress curves for hot rolled steel at various temperatures (Chen & Young, 2006) b Thermal expansion of steel, mentioned in EN 1992–1–2:2005 Eurocode 2 c Specific heat changes of steel (Franssen & Real, 2012) d Thermal conductivity of steel (Franssen & Real, 2012)

integration points were considered along with each beam-column element. At each of these sections, the fibers have a bilinear stress–strain curve modeled using Steel02Thermal materials. Considering the expansion coefficient of steel at different temperatures, coefficient of resistance reduction will be automatically applied by software following the EN 1993–1–1 (2005) standard.

Modeling of the beams was done in two ways; in the beams exposed to heating, the beams were modeled similar to the columns with a dispBeamColumnThermal element in the software.

In this case, the beams were divided into five segments, and five integration points were considered along with the beam-column element.

Whereas in the beams not exposed to heat, inelastic behavior of the beams were modeled as concentrated plasticity considering two nonlinear rotational springs at two

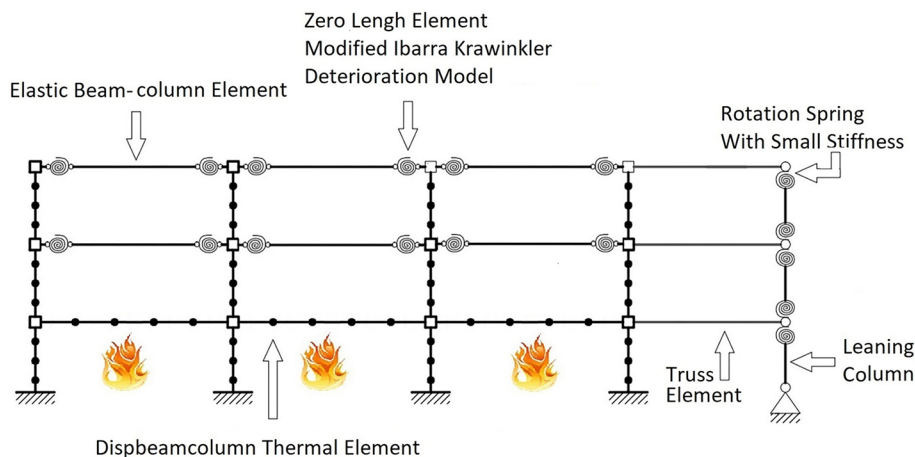
ends and an elastic beam-column element between them in the form of a series.

The nonlinear behavior of the rotational springs was determined using a modified Ibarra-Medina-Krawinkler (IMK) model, and the parameters for this model were calculated using the equations presented by Lignos and Krawinkler (2011).

The second-order (P-delta) effects of gravity columns were considered using the leaning column (Fig. 3).

As can be seen in Fig. 3, the leaning column was modeled using beam-column elements with a large moment of inertia and broad cross-Sect. (100 times the cross-section and moment of inertia of the most substantial gravitational column) connected to nodes in the alignment of stories using a rotational spring with small stiffness (Khorasani et al., 2015).

**Fig. 3** Schematic of frame modeling in OpenSees software for seismic and thermal analysis considering the fire scenario in the first floor



Each of these nodes is connected to the frame by a rigid truss. Given that the structures have two resisting frames in lateral load direction (Venture & Sacramento, 1994), the gravity load share of half of the non-bearing lateral columns of each story has been applied to the leaning column on that story.

The rigid elements were also used in the beams and columns to consider the end areas of the rigid beams and columns. The length of each of the rigid elements in the beam and column is half the height of the cross-section. The rigid trusses were used for the roof diaphragm in the model, which were removed after that the seismic loading was completed on the roofs exposed to heat.

### 5 Seismic Loading

In seismic loading, far-field acceleration mapping scales for seven earthquakes, according to Table 1, taken from the Pacific Earthquake Engineering Research Center (PEER) database (PEER, 2014) and FEMA P-695 (2009), and scaled to the performance level of life safety were applied to the structure.

According to the structural analysis at the macro-scale, the relative displacement of the stories has been investigated.

The relative displacement of the stories following FEMA356 (2000) was assumed to be 2.5% of the Steel Moment Frame in the life safety performance level.

Thus, Earthquake scales in which maximum relative displacement of stories under its affected structure is less than 2.5% were applied to the structure.

As mentioned earlier, the design details of the structure are available in FEMA 355C (Krawinkler, 2000). Dynamic analysis was performed on the designed structure under different earthquake scales and the value of the engineering demand parameter for the structure, which is the maximum inter story drift in this research, is obtained. The steps of scaling the earthquake, analyzing the time history and obtaining the engineering parameter continue to the level of life safety.

### 6 Thermal Loading

Several methods have been developed to calculate the thermal performance of a fire inside a compartment. These methods are either based on laboratory studies, using parametric fires known as "temperature and time curves" as stated in International Standards of ISO 834 (1999) and ASTM E119 (2006), or as stated in SEI and ASCE (2005), they follow "natural

**Table 1** Set of 7 records selected for analysis

Earthquake				Recording station	
Number	Name	Year	Magnitude (M)	Name	Record file name
1	Manjil, Iran	1990	7.4	Abbar	ABBAR-L
2	Duzce, Turkey	1999	7.1	Bolu	BOL000
3	Landers	1992	7.3	Cool water	CLW-LN
4	Northridge	1994	6.7	Canyon Country-WLC	LOS000
5	Northridge	1994	6.7	Beverly Hills-Mulhol	MUL009
6	San Fernando	1971	6.6	LA-Hollywood Stor	PEL090
7	Friuli, Italy	1976	6.5	Tolmezzo	A-TMZ000

fires” that are primarily a function of the volume of gas produced by combustible materials in a covered space (Behnam & Ronagh, 2013).

The cooling phase is based on the assumption that, after a period of fire, there will be less air or combustible materials available; thereby, the temperature or load of the fire will be reduced.

This assumption about fire only is more realistic, considering that the openings are closed. However, in buildings that had been previously damaged by the earthquake, the window is likely to break, so the pattern of fire progression is different from that of "natural" fire.

Consequently, it is strongly recommended to use a non-cooling phase curve (Tanaka et al., 1998) for the fire load at the time of PEF.

For this research, a temperature–time curve of ISO 834 was used without the cooling phase, and the temperature–time relation is based on Eq. 1 (Behnam & Ronagh, 2013):

$$T = 345 \log_{10}(8t + 1) + T_0 \quad (1)$$

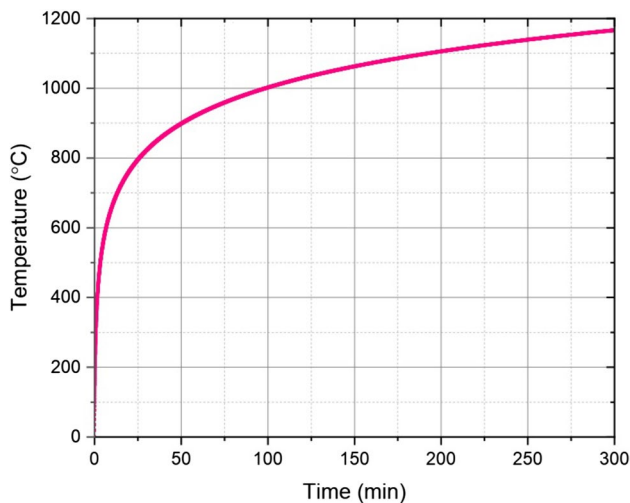


Fig. 4 Fire curve according to ISO 834

where  $t$  is the time in minutes, and  $T_0$  and  $T$  are ambient temperatures and temperature at time  $t$  in degrees Celsius, respectively (Fig. 4).

In this study, to apply the thermal load, the fire load of 1.6 s to a duration of 880 s (i.e. 550 steps) is assumed considering loading steps. This means that the fire will be overcome after 880 s and the structure behavior will be controlled for this duration of fire for various earthquake scales up to the life safety level.

According to Fig. 5, three scenarios are considered for thermal loading in the present study. In the first scenario, only the first story was subjected to a fire of up to 880 s under the ISO834 fire curve, meaning that, after this time the fire has been extinguished, while in the second scenario, the first and second stories were simultaneously exposed to a fire of up to 880 s under this curve, and in the third scenario all stories were simultaneously exposed to a fire of up to 880 s under this curve.

The heat transfer model is often used to predict temperature profiles of structural steel members under standard and natural fire conditions assuming full fire extension.

Since the effect of convective heat transfer is small, so, the convective heat transfer coefficient of 20–25 ( $\text{W}\cdot\text{m}^{-2}\cdot\text{k}^{-1}$ ) is recommended (Ghojel & Wong, 2005), which is considered equal to 25 ( $\text{W}\cdot\text{m}^{-2}\cdot\text{k}^{-1}$ ) in this study.

Heat transfer in beams and columns within the fire compartment can be modeled concerning exposed faces of the profile fire, in the closed-form solution by considering several masses concentrated at the cross-section of the profile for states of no slab (Quiel & Garlock, 2010) and with concrete slab (Ghojel & Wong, 2005) on beam (Fig. 6).

As can be seen in Fig. 6, in these states, the web and flanges are considered as concentrated masses, and the heat transfer occurs between the points using the law of energy conservation. As shown in Fig. 6, heat transfer is specified from the fire to concentrate masses exposed to fire ( $Q_{in}$ ) as well as heat transfer of concentrated mass to the ambient temperature or concrete slab ( $Q_{out}$ ) and heat transfer between considered concentrated masses ( $Q_{1-2}$ ,  $Q_{2-3}$ , and  $Q_{2-4}$ ). When the strong axis is exposed to fire, three lumped masses are considered, while a total of seven lumped masses are considered, in the case that the weak

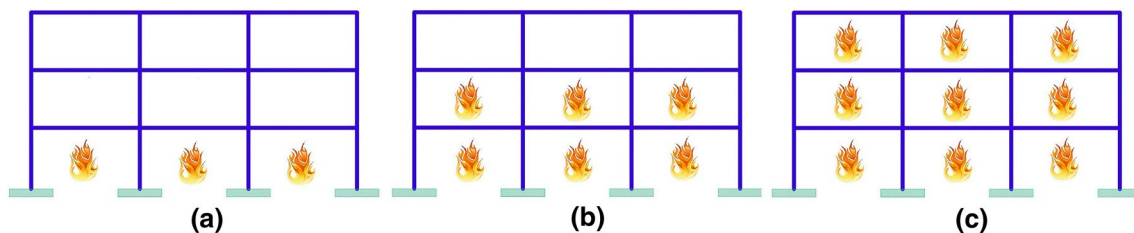
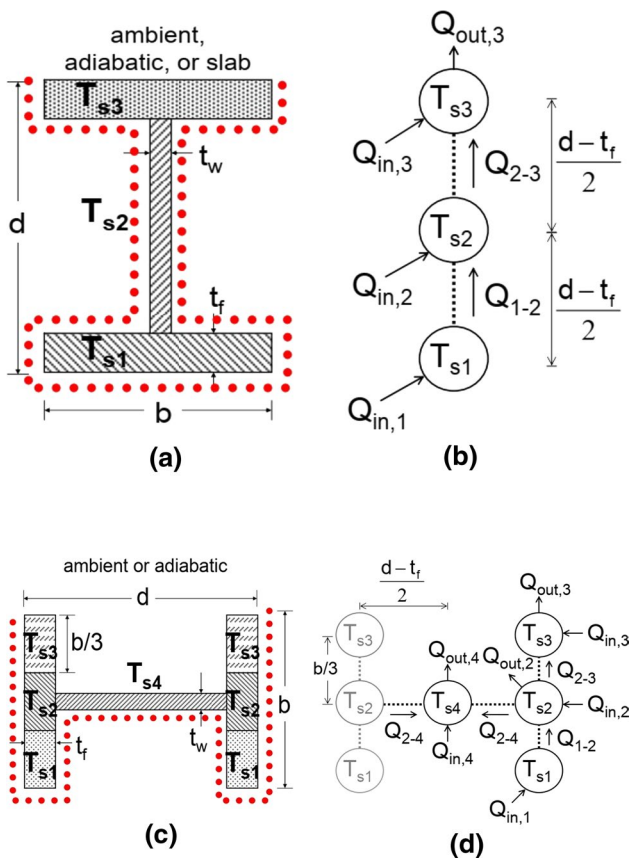


Fig. 5 Fire scenarios in selected models: **a** Scenario 1; **b** Scenario 2; **c** Scenario 3



**Fig. 6** Closed-form methodology for thermal analysis: **a** The strong axis of the cross-section with 3-sided fire exposures **b** an equivalent system of lumped masses for strong axis **c** Weak axis of the cross-section with 3-sided fire exposures **d** an equivalent system of lumped masses for weak axis (Quiel & Garlock, 2010)

axis is exposed to fire, among which the three masses on the flanges are common.

Due to addition of heat transfer modules in the OpenSees software, it is possible to perform heat transfer analysis in this software. Therefore, through meshing of the profiles according to Figs. 7, 9-point heat transfer analysis was performed using the finite element method of solving the transient governing equations in the software.

### 6.1 Validation of Heat Transfer Analysis

To validate heat transfer in the OpenSees software, beam profile of UB 82.0 530 (no slab) (Lewis, 2000) exposed to standard fire on three sides was meshed in the OpenSees software and was subjected to heat transfer analysis, and then the results of maximum, average, and minimum temperature of profiles at different times were compared using the SAFIR software (Fig. 8).

As shown in Fig. 8, heat transfer results of the two softwares are similar at the average and maximum temperature of the profiles.

Therefore, in structural heat analysis in the OpenSees software, to account for the thermal gradient of the profile, the maximum temperature at different points at 9 points in the profile height was applied in the form of the thermal load to the beams and columns exposed to fire.

Since the radioactive component of heat transfer, The values of the Stefan-Boltzmann constant and the emissivity of carbon steel were considered equal  $5.67 \times 10^{-8}$  ( $W.m^{-2}.K^{-4}$ ) (Ghojel & Wong, 2005) and 0.7 (EN 1993-1-1, 2005) respectively. They were used as input data for heat transfer by software.

### 6.2 Validation of PEF Analysis with Experimental Results

For validation of thermal analysis in OpenSees software, the steel frame ZSR1 (Rubert & Schaumann, 1986) is loaded according to Fig. 9 and the dead weight of the beams is widely considered to be 60 Newton per meter on the beams.

The frame sections are IPE80 with ST37 steel and the yield stress and modulus of elasticity at the ambient temperature of the frame are 355 MPa and 210,000 MPa, respectively. As shown in Fig. 9, the specified beams and columns are heated uniformly until the frame is stable. Using Steel02Thermal materials in OpenSees software, I-shaped sections with 8 fibers in the web and 4 fibers in each flange are modeled. A comparison between the horizontal displacement at the point specified in Fig. 9 shows that the software analysis results are consistent with the test results (Fig. 10).

Considering the application of horizontal load in this model along with thermal loading, the model can be validated for PEF with laboratory results.

### 7 Discussion

For post-earthquake fire analysis, as mentioned, 60 s of free vibration is assumed to dampen the structure. Figure 11 shows horizontal displacement of node A under the scaled accelerogram of Manjil earthquake (Abbar station) for  $Sa(T1)$  equal to 0.81 g and then applying 60 s of free vibration after that and then fire for up to 880 s in the first and second floors (Scenario 2).

Considering that this permanent deformation is different in various earthquakes, in continuous seismic-thermal analysis, the effect of this deformation is considered in various points.

As explained in the previous sections, in this study, post-earthquake fire analysis was performed on a 3-story

**Fig. 7** Meshing of the cross-section profiles and heat gradient points for heat transfer analysis in the OpenSees software

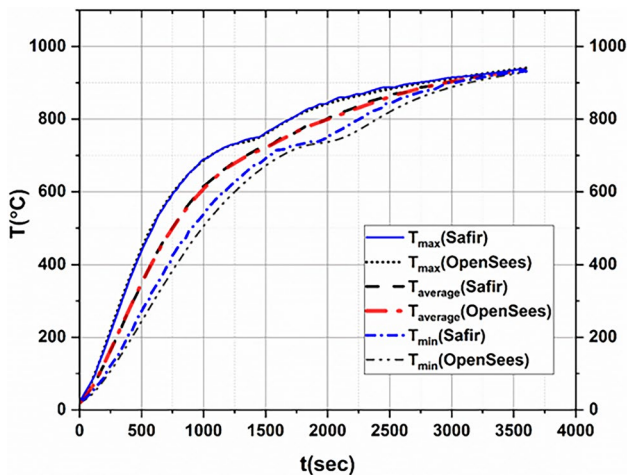
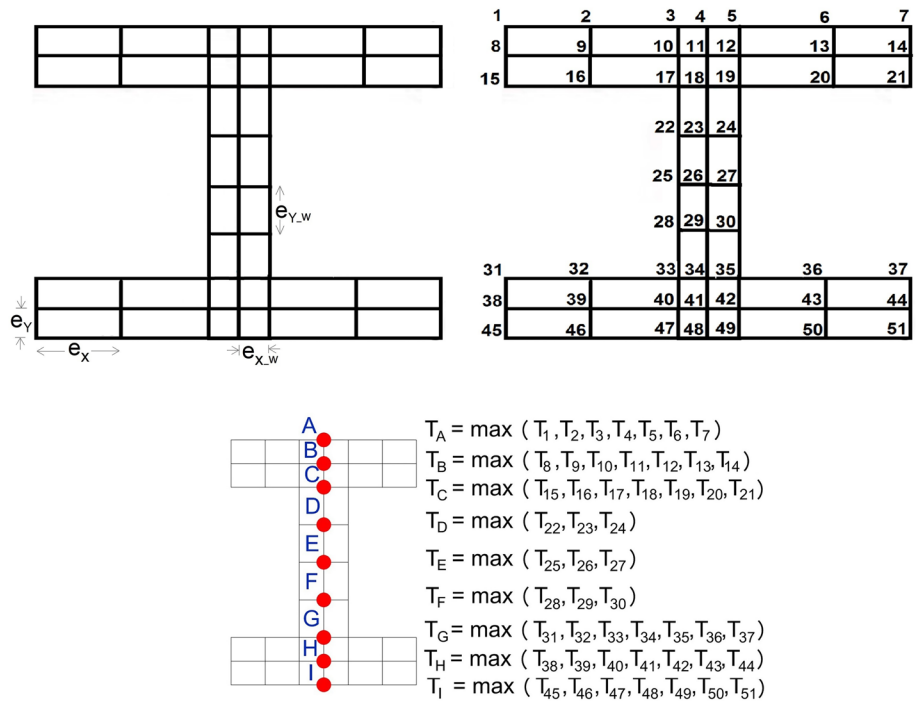


**Fig. 8** Maximum, average, and minimum temperatures of a 530 UB 82.0 beam profile exposed on three sides to the ISO 834 fire curve (no slab)

SAC structure under different earthquake scales and 880 s of fire after that for various fire scenarios.

From the analysis results, considering seven accelerograms and three fire scenarios, a total of 21 graphs could be drawn. Due to space limitation and similar trend of diagrams, three accelerometers are selected from seven accelerograms to draw the graphs. Figures 12, 13, 14, 15, 16, 17, 18, 19, 20 show the results of post-earthquake fire analysis in a 3-story SAC structure under different scales

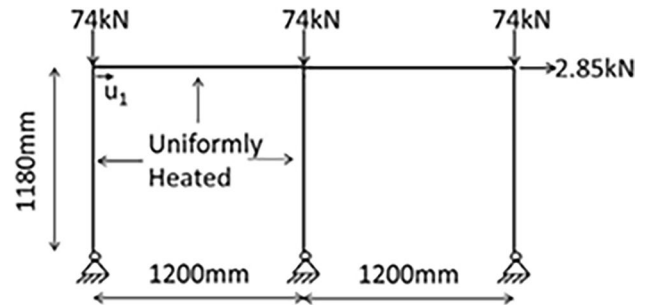


**Fig. 9** Configuration of ZSR1 Frame (Rubert & Schaumann, 1986)

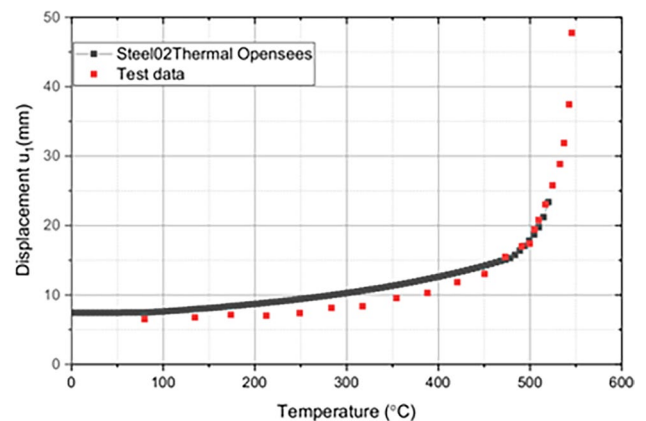


**Fig. 10** Comparison of  $u_1$  laboratory displacement with OpenSees software results



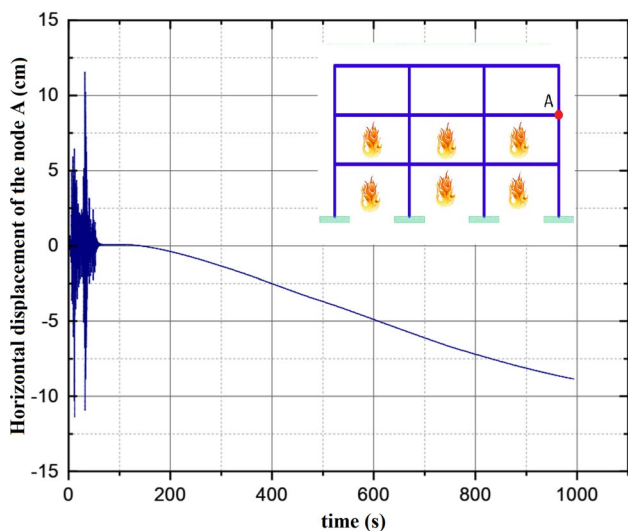


**Fig. 11** Horizontal displacement of node A under the scaled accelerogram of Manjil earthquake (Abbar station) with  $Sa(T1)$  equal to 0.81 g and then fire in Scenario 2 for to 880 s

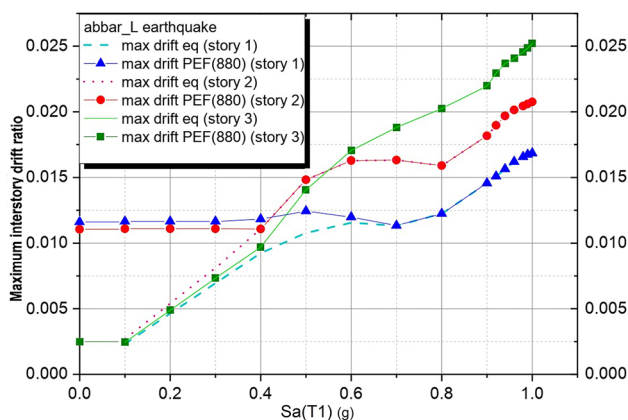


**Fig. 12** Maximum relative drift of the stories in the three-story SAC structure under different acceleration mapping scales in the Abbar station of Manjil and fire scenario 1

of the selected accelerogram and 880 s of fire after that for various fire scenarios.

According to the applied earthquake records and the period of the structure, the acceleration spectrum component in the period of the first mode of the structure  $Sa(T1)$  is obtained. In each step, the earthquake record is multiplied by a scale and the corresponding  $Sa(T1)$  is obtained. By increasing the record scale coefficient and then by increasing  $Sa(T1)$ , the steps are continued until reaching the level of life safety under earthquake (maximum relative displacement between stories of 2.5% according to FEMA356) and in each step, the fire load is applied to the structure up to 880 s of fire in accordance with the ISO 834 curve.

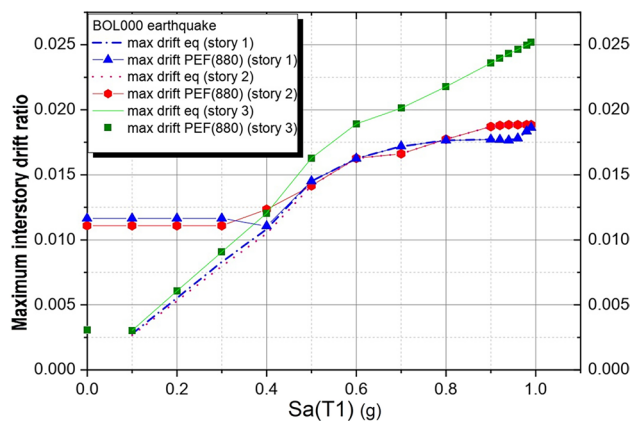


**Fig. 13** Maximum relative drift of the stories in the three-story SAC structure under different acceleration mapping scales in the Bolu station of Duzce and fire scenario 1

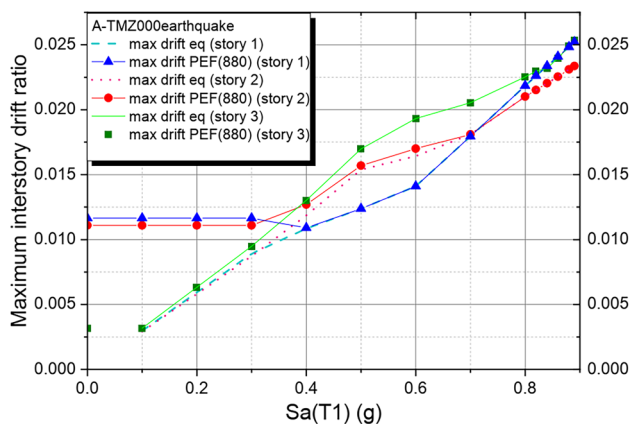


**Fig. 14** Maximum relative drift of the stories in the three-story SAC structure under different acceleration mapping scales in the Tolmezzo station of Friuli and fire scenario 1

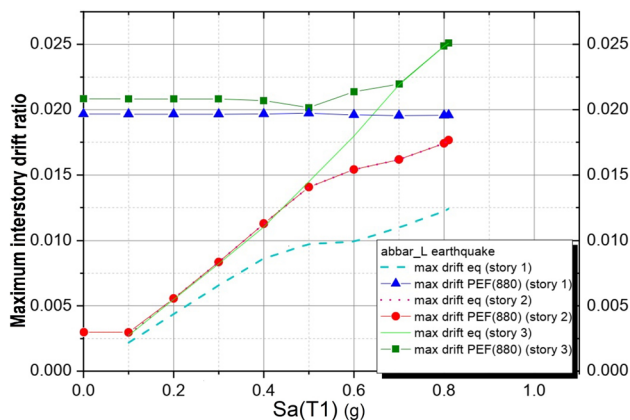


**Fig. 15** Maximum relative drift of the stories in the three-story SAC structure under different acceleration mapping scales in the Abbar station of Manjil and fire scenario 2

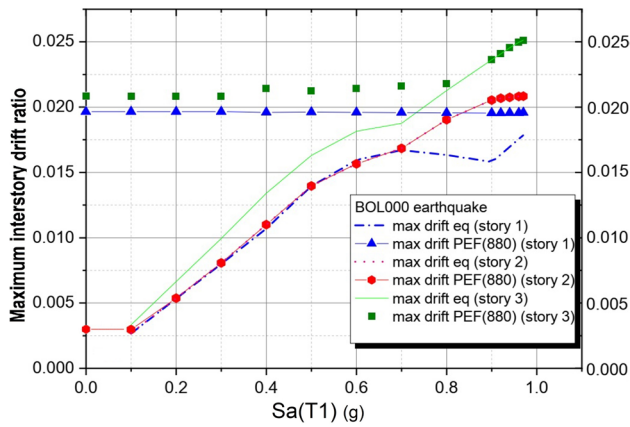


**Fig. 16** Maximum relative drift of the stories in the three-story SAC structure under different acceleration mapping scales in the Bolu station of Duzce and fire scenario 2

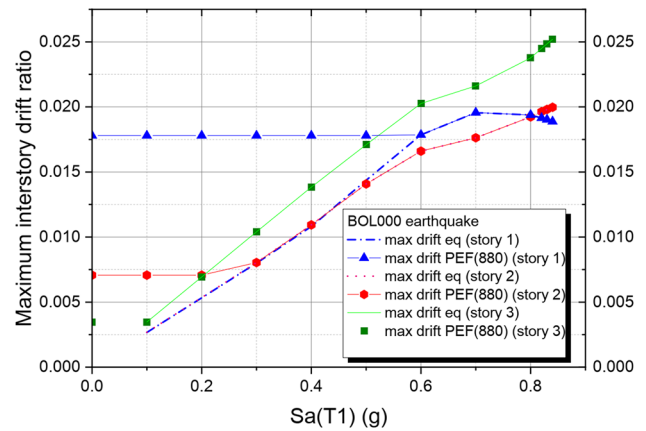


**Fig. 19** Maximum relative drift of the stories in the three-story SAC structure under different acceleration mapping scales in the Bolu station of Duzce and fire scenario 3

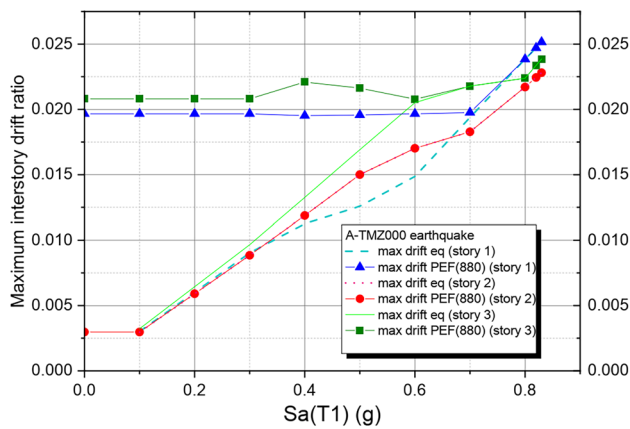


**Fig. 17** Maximum relative drift of the stories in the three-story SAC structure under different acceleration mapping scales in the Tolmezzo station of Friuli and fire scenario 2

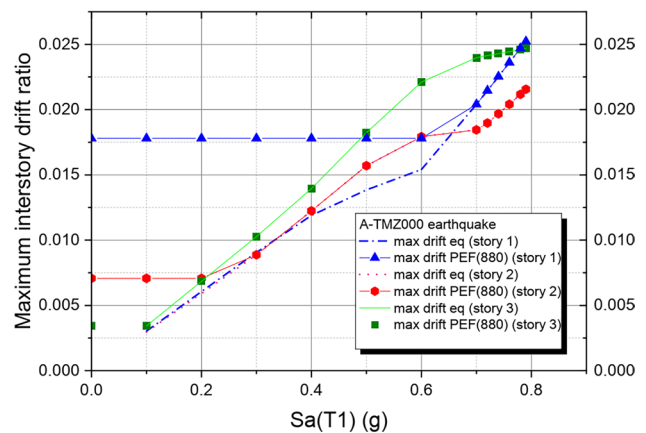


**Fig. 20** Maximum relative drift of the stories in the three-story SAC structure under different acceleration mapping scales in the Tolmezzo station of Friuli and fire scenario 3

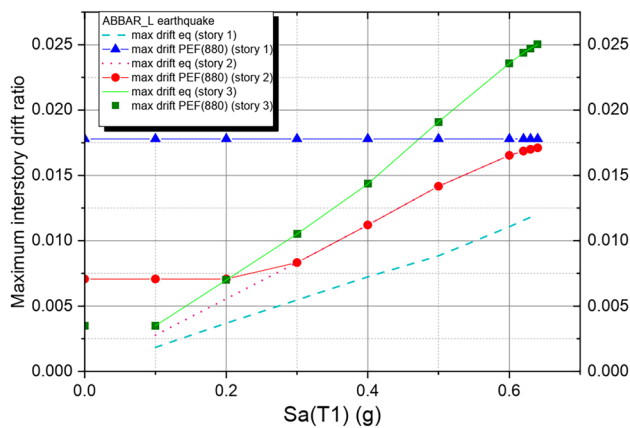


**Fig. 18** Maximum relative drift of the stories in the three-story SAC structure under different acceleration mapping scales in the Abbar station of Manjil and fire scenario 3

For example, as shown in Fig. 12, the structure was subjected to different scales of earthquake recorded at Abbar station of Manjil, and then the first story was heated for 880 s. It was observed that, until the occurrence of pseudo-acceleration spectral component at the primary mode of the structure period ( $S_a(T_1)$ ), which is equal to 0.7 g, relative displacement of the first story is more critical at the PEF case than the earthquake-only case, whereas it occurs at the ( $S_a(T_1)$ ) = 0.4 g in the second story. In the third story, relative displacement of the story exposed to the PEF at different scales is entirely consistent with the earthquake-only case showing that the PEF is not critical on the relative displacement of this story.

Also, for  $S_a(T_1)$  above 0.4 g as shown in the Fig. 12, the structure has been shown nonlinear behavior in the first story under post-earthquake fire analysis. Figures 13, 14,

15, 16, 17, 18, 19, 20 can also be analyzed in accordance with Fig. 12.

The structure in question was also studied under 880 s of fire alone. The results of the analysis showed that the maximum relative displacement between stories is the same in fire alone and fire with mild earthquakes. Therefore, in Figs. 12, 13, 14, 15, 16, 17, 18, 19, 20, the maximum relative displacement between stories in Sa(T1) is zero, similar to the values of Sa(T1) is 0.1 g.

Examining the three considered fire scenarios, it was found that in the case of 880 s of fire alone, the maximum

relative displacement between the stories under scenarios 1, 2 and 3 is 0.0116, 0.0208 and 0.0177, respectively. It turns out that scenario 2 of fire in this structure is more critical under the studied fire scenarios.

Tables 2, 3, 4 present the results of the analysis of seven earthquake records for scenarios of fire. In the last column of these tables the averages the results have been calculated.

According to the results presented in Tables 2, 3, 4, the results of the PEF analysis can be different concerning the scale of an applied earthquake; the structure will experience different maximum relative displacement in different

**Table 2** Comparison of modeling results for fire scenario 1

Record file name		ABBAR-L	BOL000	CLW-LN	Sa(T1)				Average
					LOS000	MUL009	PEL090	A-TMZ000	
Story 1	PEF	<0.7 g	<0.5 g	<0.5 g	<0.7 g	<0.6 g	<0.5 g	<0.4 g	<0.557 g
	Eq	>0.7 g	>0.5 g	>0.5 g	>0.7 g	>0.6 g	>0.5 g	>0.4 g	>0.557 g
Story 2	PEF	<0.4 g	<0.5 g	<0.5 g	<0.4 g	<0.4 g	<0.6 g	<0.7 g	<0.5 g
	Eq	>0.4 g	>0.5 g	>0.5 g	>0.4 g	>0.4 g	>0.6 g	>0.7 g	>0.5 g
Story 3	PEF	–	–	–	–	–	–	–	–
	Eq	For all	For all	For all	For all	For all	For all	For all	For all
Nonlinear behavior under PEF	Sa	>0.4 g	>0.3 g	>0.2 g	>0.4 g	>0.3 g	>0.3 g	>0.3 g	>0.31 g
	At story	At story 1	At story 2	At story 1 and story 2	At story 1	At story 1	At story 1 and story 2	At story 2	At story 1 or story 2

**Table 3** Comparison of modeling results for fire scenario 2

Record File Name		ABBAR_L	BOL000	CLW-LN	Sa(T1)				Average
					LOS000	MUL009	PEL090	A-TMZ000	
Story 1	PEF	For all	For all	<0.7 g	For all	<0.9 g	For all	<0.8 g	In most cases it is controlled by PEF
	Eq	–	–	>0.7 g	–	>0.9 g	–	>0.8 g	
Story 2	PEF	–	–	–	–	–	–	–	–
	Eq	For all	For all	For all	For all	For all	For all	For all	For all
Story 3	PEF	<0.7 g	<0.8 g	<0.6 g	<0.8 g	<0.96 g	<0.6 g	<0.7 g	<0.73 g
	Eq	>0.7 g	>0.8 g	>0.6 g	>0.8 g	>0.96 g	>0.6 g	>0.7 g	>0.73 g
Nonlinear behavior under PEF	Sa	>0.4 g	>0.3 g	>0.2 g	>0.4 g	>0.5 g	>0.3 g	>0.3 g	>0.34 g
	At story	At story 3	At story 3	At story 3	At story 3	At story 3	At story 3	At story 3	At story 3

**Table 4** Comparison of modeling results for fire scenario 3

Record file name		ABBAR_L	BOL000	CLW-LN	Sa(T1)				Average
					LOS000	MUL009	PEL090	A-TMZ000	
Story 1	PEF	For all	<0.5 g	<0.5 g	For all	<0.8 g	<0.5 g	<0.6 g	<0.58 g
	Eq	–	>0.5 g	>0.5 g	–	>0.8 g	>0.5 g	>0.6 g	>0.58 g
Story 2	PEF	<0.2 g	<0.2 g	<0.2 g	<0.2 g	<0.2 g	<0.2 g	<0.2 g	<0.2 g
	Eq	>0.2 g	>0.2 g	>0.2 g	>0.2 g	>0.2 g	>0.2 g	>0.2 g	>0.2 g
Story 3	PEF	–	–	–	<0.1 g	<0.1 g	–	–	In most cases it is controlled by Eq
	Eq	For all	For all	For all	>0.1 g	>0.1 g	For all	For all	
Nonlinear behavior under PEF	–	–	–	–	–	–	–	–	–

stories relative to the earthquake-only case. At some levels of applied earthquake, maximum relative displacement experienced by the structure under the earthquake is higher than the time that the PEF occurs. For instance, in the third story of the first fire scenario under the Abbar earthquake, it is quite clear that the structure will experience a more significant maximum relative displacement of the account under the earthquake-only case. While, the state of this story will be critical in the second fire scenario under the Abbar earthquake with ( $S_a(T1)$ ) smaller than 0.7 g in the PEF case, and the structure will experience maximum relative displacement for earthquakes with ( $S_a(T1)$ ) higher than 0.7 g under the earthquake alone.

As shown in Figs. 8, 9, 10, 11, in the initial  $S_a(T1)$ , post-earthquake fire, due to the mildness of the earthquake, cause more maximum relative displacement between stories than the earthquake alone. Examining the maximum relative displacement between the stories in this case according to the last row of Tables 2, 3, 4, it is found that in Scenario 1 under 880 s of post-earthquake fire on average of  $S_a(T1)$  greater than 0.31 g in the first or second story, the relative maximum of the stories under PEF changes and the structure exhibits nonlinear behavior in PEF mode.

However, in Scenario 2 of fire on average in  $S_a(T1)$  greater than 0.34 g, this nonlinear behavior is seen in the structure under PEF, and in Scenario 3, considering that three stories are under fire at the same time, the displacement of the stories under post-earthquake fire become more uniform, and the structure under earthquake alone is more critical, and the onset of nonlinear behavior under PEF is not seen.

## 8 Conclusions

The main objective of this paper is to study the behavior of moment steel frame structures under post-earthquake fire for various earthquake scales up to the life safety level. If a structure is designed for a certain  $S_a(T1)$  under an earthquake and under that earthquake scale it is at a certain level of performance, in the event of a post-earthquake fire it may go beyond that level of performance. Due to the possibility of designing structures for different  $S_a(T1)$ , their performance in post-earthquake fires may vary.

In the present study, the 3-story SAC structure was analyzed under different earthquake scales up to the level of life safety, and after free vibration, the thermal load was applied to the structure by the fire curve of ISO 834–880 s. PEF analysis was performed for three fire scenarios including fire on the first story (Scenario 1) and fire on the first and second stories simultaneously (Scenario 2) and fire on all stories simultaneously (Scenario 3).

Comparing the results, it was found that the structure creates more relative displacement between stories under the PEF in scenario 2, and in this scenario, the post-earthquake fire is critical in all earthquake scenarios up to the level of life safety under 880 s of fire. However, in scenario 1 and scenario 3, if the  $S_a(T1)$  of the structure under the earthquake record is greater than about 0.6 g and the structure is at a certain level of performance, in case of 880 s of post-earthquake fire, it will remain at that level and controlling the structure for PEF in this duration of fire does not considerably affect the results.

## References

- ASCE. (2005). Minimum design loads for buildings and other structures: SEI/ ASCE 7–05. In 2005: ASCE Reston.
- ASTM. (2006). Standard test methods for determining effects of large hydrocarbon pool fires on structural members and assemblies. *ASTM E1529–06*. <https://www.astm.org/DATABASE.CART/HISTORICAL/E1529-06.htm>.
- Behnam, B. (2016). Structural response of vertically irregular tall moment-resisting steel frames under pre-and post-earthquake fire. *The Structural Design of Tall and Special Buildings*, 25(12), 543–557.
- Behnam, B. (2017). *Post-earthquake fire analysis in urban structures: Risk management strategies*. CRC Press.
- Behnam, B. (2018). Failure sensitivity analysis of tall moment-resisting structures under natural fires. *International Journal of Civil Engineering*, 16(12), 1771–1780.
- Behnam, B., & Ronagh, H. (2013). A post-earthquake fire factor to improve the fire resistance of damaged ordinary reinforced concrete structures. *Journal of structural fire engineering*. <https://doi.org/10.1260/2040-2317.4.4.207>
- Chen, J., & Young, B. (2006). Stress–strain curves for stainless steel at elevated temperatures. *Engineering Structures*, 28(2), 229–239.
- Della Corte, G., Landolfo, R., & Mazzolani, F. (2003). Post-earthquake fire resistance of moment resisting steel frames. *Fire Safety Journal*, 38(7), 593–612.
- EN 1993–1–1 (2005). Eurocode 3: Design of steel structures - Part 1-1: General rules and rules for buildings [Authority: The European Union Per Regulation 305/2011, Directive 98/34/EC, Directive 2004/18/EC]
- FEMA. (2000). *Prestandard and commentary for the seismic rehabilitation of buildings (FEMA356)* (p. 7). Federal Emergency Management Agency.
- FEMA, P 695 (2009). *Quantification of building seismic performance factors*: US Department of Homeland Security.
- Franssen, J.-M., & Gernay, T. (2019). *User's manual for SAFIR 2019 A computer program for analysis of structures subjected to fire*. University of Liege, Department ArGenCO, Service Structural Engineering.
- Franssen, J.-M., & Real, P. V. (2012). *Fire design of steel structures: Eurocode 1: Actions on structures; Part 1–2: General actions–Actions on structures exposed to fire; Eurocode 3: Design of steel structures; Part 1–2: General rules—Structural fire design*. Wiley.
- Ghojel, J. I., & Wong, M. (2005). Three-sided heating of I-beams in composite construction exposed to fire. *Journal of Constructional Steel Research*, 61(6), 834–844.
- International Standard ISO 834–1 (1999). Fire Resistance Tests - Elements of Building Construction - Part 1: General Requirements

- Khorasani, N. E., & Garlock, M. E. (2017). Overview of fire following earthquake: Historical events and community responses. *International Journal of Disaster Resilience in the Built Environment*. <https://doi.org/10.1108/IJDRBE-02-2015-0005>
- Khorasani, N. E., Garlock, M. E., & Quiel, S. E. (2015). Modeling steel structures in OpenSees: Enhancements for fire and multi-hazard probabilistic analyses. *Computers and Structures*, 157, 218–231.
- Krawinkler, H. (2000). State of art report on systems performance of moment resisting steel frames subject to earthquake ground shaking. *FEMA 355c*.
- Lewis, K. R. (2000). Fire design of steel members.
- Lignos, D. G., & Krawinkler, H. (2011). Deterioration modeling of steel components in support of collapse prediction of steel moment frames under earthquake loading. *Journal of Structural Engineering*, 137(11), 1291–1302.
- Mazzoni, S., McKenna, F., Scott, M. H., & Fenves, G. L. (2006). OpenSees command language manual. *Pacific Earthquake Engineering Research (PEER) Center*, 264. <https://opensees.berkeley.edu/OpenSees/manuals/usermanual/index.html>.
- Memari, M., Mahmoud, H., & Ellingwood, B. (2014). Post-earthquake fire performance of moment resisting frames with reduced beam section connections. *Journal of Constructional Steel Research*, 103, 215–229.
- PEER. (2014). *PEER NGA-West2 database, PEER report 2013/03*. Berkeley: University of California.
- Quiel, S. E., & Garlock, M. E. (2010). Closed-form prediction of the thermal and structural response of a perimeter column in a fire. *The Open Construction and Building Technology Journal*. <https://doi.org/10.2174/1874836801004010064>
- Rubert, A., & Schaumann, P. (1986). Structural steel and plane frame assemblies under fire action. *Fire Safety Journal*, 10(3), 173–184.
- Ryder, N. L., Wolin, S. D., & Milke, J. A. (2002). An investigation of the reduction in fire resistance of steel columns caused by loss of spray-applied fire protection. *Journal of Fire Protection Engineering*, 12(1), 31–44.
- SAP C. (2009). *Version 14 Integrated finite element analysis and design of structures Basic analysis references manual*. Computers and Structures Inc.
- Systèmes, D. (2007). Abaqus analysis user's manual. *Simulia Corp. Providence, RI, USA*. [http://130.149.89.49:2080/v6.10/pdf\\_books/ANALYSIS\\_3.pdf](http://130.149.89.49:2080/v6.10/pdf_books/ANALYSIS_3.pdf)
- Tanaka, T., Hagiwara, I., Harada, K., Ohmiya, Y., Mizuno, M., Yamaguchi, J., et al. (1998). Performance-based fire safety design of a high-rise office building. In *Proceedings of the Second International Conference on Performance-Based Codes and Fire Safety Design Methods*, Building Research Institute. Japan.
- Tomecek, D. V., & Milke, J. A. (1993). A study of the effect of partial loss of protection on the fire resistance of steel columns. *Fire Technology*, 29(1), 3–21.
- UBC, B. S. S. C. (1994). Edition NEHRP Recommended Provisions for Seismic Regulations for New Buildings. Issued by FEMA in furtherance of the Decade for Natural Disaster Reduction, *Federal Emergency Management Agency*.
- Venture, S. J., & Sacramento, C. (1994). Invitational workshop on steel seismic issues. *Proc., Rep. SAC*, 94, 1.
- Wang, W.-Y., & Li, G.-Q. (2009). Fire-resistance study of restrained steel columns with partial damage to fire protection. *Fire Safety Journal*, 44(8), 1088–1094.
- Zaharia, R., & Pintea, D. (2009). Fire after earthquake analysis of steel moment resisting frames. *International Journal of Steel Structures*, 9(4), 275–284.

**Publisher's Note** Springer Nature remains neutral with regard to jurisdictional claims in published maps and institutional affiliations.